ORIGINAL ARTICLE

CrossMark

MiR-6872 host gene SEMA3B and its antisense lncRNA SEMA3B-AS1 function synergistically to suppress gastric cardia adenocarcinoma progression

Wei Guo[1] · Xiaoliang Liang[1] · Lei Liu[2] · Yanli Guo[1] · Supeng Shen[1] · Jia Liang[1] · Zhiming Dong[1]

Abstract

Background Semaphorin 3B (SEMA3B) is frequently inactivated in several carcinomas. However, as the host gene of miR-6872, the roles of SEMA3B, antisense lncRNA SEMA3B-AS1, and miR-6872 in gastric cardia adenocarcinoma (GCA) tumorigenesis have not been clarified.

Methods The expression levels of SEMA3B, SEMA3B-AS1, and miR-6872 were respectively detected by qRT-PCR, western blot, or immunohistochemical staining assays. The methylation status was determined by BGS and BS-MSP methods. In vitro assays were preformed to explore the biological effects of SEMA3B, SEMA3B-AS1, and miR-6872-5p in gastric cancer cells. Chromatin immunoprecipitation assay was used to detect the binding of protein to DNA. The interaction of SEMA3B-AS1 with MLL4 was identified by RNA immunoprecipitation and RNA pull-down assays.

Results Frequent downregulation of SEMA3B, SEMA3B-AS1, and miR-6872 was detected in GCA tissues and gastric cancer cells. Aberrant hypermethylation of the promoter region was more tumor specific and was negatively correlated with the expression level of SEMA3B, SEMA3B-AS1, and miR-6872-5p. Transcription factor Sp1 activated SEMA3B or SEMA3B-AS1 transcription and CpG sites hypermethylation within promoter region eliminated Sp1 binding ability. Overexpression of SEMA3B and SEMA3B-AS1 inhibited gastric cancer cell proliferation, migration, and invasion in vitro. SEMA3B-AS1 induced the expression of SEMA3B by interacting with MLL4. ZNF143 might be the target gene of miR-6872-5p and miR-6872-5p functioning synergistically with SEMA3B to suppress cell invasion. Furthermore, SEMA3B, SEMA3B-AS1, and miR-6872-5p expression levels were associated with GCA patients' survival.

Conclusions SEMA3B, SEMA3B-AS1, and miR-6872 may act as tumor suppressors and may serve as potential targets for antitumor therapy.

Keywords SEMA3B · SEMA3B-AS1 · MiR-6872 · Gastric cardia adenocarcinoma · Expression

✉ Zhiming Dong
dongzhiming2000@163.com

1 Laboratory of Pathology, Hebei Cancer Institute, The Fourth Hospital of Hebei Medical University, Jiankang Road 12, Shijiazhuang 050011, Hebei, China

2 Department of Thoracic Surgery, The Fourth Hospital of Hebei Medical University, Shijiazhuang, Hebei, China

Background

Gastric cardia adenocarcinoma (GCA) was formerly considered as esophageal cancer or gastric cancer. However, due to the distinct epidemiological and biological characteristics and improvement in classification, GCA has been diagnosed independently in recent years [1]. Despite the worldwide steady decline in the incidence and mortality of noncardia gastric cancer, the incidence of GCA is on the rise both in developing and developed countries during the past few decades [2]. About 50% of stomach adenocarcinomas now diagnosed in the developed countries arise from the cardia region [3]. In China, the incidence of GCA has increased gradually in the past few years, especially in some rural areas bordering Taihang Mountains including Cixian and

Springer

Shexian of Hebei Province, Linxian of Henan Province [4]. *Helicobacter pylori* infection is the strongest identified risk factor for noncardia gastric cancer [5]; in contrast, the exact risk factors and etiology for GCA still remain unclarified.

Loss of heterozygosity (LOH) on the chromosome 3p is one of the most frequent events in a variety of human epithelial tumors [6] and may influence the expression of several potential tumor suppressor genes (TSGs) located at the region, such as RASSF1A, BLU, hMLH1 at 3p21.3 [7], FHIT at 3p14 [8], and DUTT1 at 3p12 [9]. Our previous study has detected downregulation and promoter hypermethylation of RASSF1A in GCA [10]. It is necessary to study the roles of other TSGs at this region in GCA tumorigenesis. Semaphorin 3B (SEMA3B), located on 3p21.3, is frequently inactivated in several types of carcinomas [11–15]. SEMA3, the only secreted soluble molecules of semaphorins family, was first identified as glycoproteins that negatively mediate neuronal guidance by binding to neuropilin and repelling neurons away from the source of SEMA3 [16]. The following studies have demonstrated that SEMA3B play inhibitory roles in tumor proliferation and angiogenesis [17]. Moreover, like other TSGs located at 3p21.3, the inactivation of SEMA3B in tumors may be caused by multiple mechanisms including allelic loss and aberrant CpG site methylation [11, 14, 15, 18–20]. However, the critical CpG sites and exact roles of SEMA3B in GCA have not been clarified.

MiR-6872 is located in the intron of SEMA3B. The genes in which these intronic miRNAs are embedded are called host genes [21]. Intronic miRNAs may co-express and play synergetic role as a partner of their host genes or play antagonistic role as an enemy and with the opposite expression level with their host genes [22]. The role of miR-6872 and its correlation with SEMA3B in tumorigenesis have not been reported. Furthermore, another long non-coding RNA (lncRNA), SEMA3B-AS1, has attracted our attention. As an antisense lncRNA, SEMA3B-AS1 has no open reading frame and coding capacity and is classified as lncRNA. LncRNAs are generally greater than 200 bp in transcript size and are associated with a series of biological processes [23, 24]. LncRNAs may play important roles in tumorigenesis [25]. Similar to protein-coding genes, lncRNA expression is subject to changes in gene dosage (e.g., copy-number alterations) and promoter utilization (e.g., DNA methylation) that occur in cancer initiation and progression [26]. A considerable amount of lncRNAs showed significant CpG island hypomethylation or hypermethylation in different kinds of tumors [27]. Hypermethylation of SEMA3B-AS1 has been detected in breast cancer [27]; however, the role and epigenetic alterations of SEMA3B-AS1 in GCA have not been reported. In the present study, we investigated the expression pattern and functional roles of SEMA3B, its antisense lncRNA SEMA3B-AS1, and miR-6872 in GCA tumorigenesis, detected the methylation status of the different regions and identified the critial CpG sites in inactivating the expression of SEMA3B, SEMA3B-AS1, and miR-6872, and further analyzed their prognostic significance in GCA tumorigenesis.

Materials and methods

Patients and specimens

One hundred and twenty-two patients with GCA (99 males, 23 females, median age 58.5 years, ranged from 37 to 72 years) undergoing surgery at the Fourth Hospital, Hebei Medical University, between the years of 2008 and 2012 were included in the present study. All gastric cardia carcinomas were adenocarcinomas with their epicenters at the gastroesophageal junction, i.e., from 1 cm above until 2 cm below the junction between the end of the tubular esophagus and the beginning of the saccular stomach [28]. Individuals with at least one first-degree relative or at least two second-degree relatives having esophageal/cardia/gastric cancer were defined as having upper gastrointestinal cancer (UGIC) family history. Information on clinical data and clinicopathologic characteristics was available from hospital recordings and pathological diagnosis. Recurrence and survival data were ascertained through the Tumor Registry and hospital chart review (Supplementary table 1). Primary GCA tissues and corresponding adjacent non-tumorous tissues were obtained from the GCA patients. Tissue samples were divided into two parallel parts, one part was formalin fixed and paraffin embedded, and the other part was frozen and stored at −80 °C to extract genomic DNA and RNA.

Cell culture and treatment

Human gastric cancer cell lines BGC-823, MGC-803, SGC-7901, HGC-27, and NCI-N87 were obtained from American Type Culture Collection (ATCC, Manassas, VA, USA) and cultured in DMEM (Gibco, Invitrogen, Life Technologies, Germany) medium under the conventional culture conditions. Cells were detected and identified as mycoplasma and free bacteria according to ATCC during the past 3 months. For drug treatment, cells were seeded at a low density and incubated for 24 h prior to treatment with DNA methyltransferase inhibitor 5-aza-2′-deoxycytidine (5-Aza-dC) or histone deacetylase inhibitor TSA. All five gastric cancer cells (2×10^5/mL) were treated either with 5 μM 5-Aza-dC (Sigma, St Louis, MO, USA) for 72 h and medium containing 5-Aza-dC was changed every 24 h or with 0.3 μM TSA (Sigma, St Louis, MO, USA) for 24 h or with the combination of 5 μM 5-Aza-dC for 48 h, followed by 0.3 μM TSA for an additional 24 h. Control cells received no drug treatment.

RNA isolation and quantitative real-time reverse transcription PCR (qRT-PCR) assay

Total RNA was isolated from cell lines, frozen tumor, and corresponding normal tissues using TRIzol reagent (Invitrogen, Carlsbad, CA, USA). For target gene expression, 2 μg RNA was used to synthesize single-stranded cDNA using the advantage RT-for-PCR kit (Clontech, Palo Alto, CA, USA). Power SYBR Green PCR Master Mix (Life Technology, Foster City, CA, USA) was used as the amplification reaction mixture. The human GAPDH gene was used as an internal control. For miR-6872-5p expression, miRcute miRNA First-strand cDNA Synthesis Kit (Tiangen, China) was used to synthesize the first strand of cDNA, and miRcute miRNA qPCR Detection Kit (SYBR Green) (Tiangen, China) was used to detect its expression. Human U6 snRNA was used for miR-6872-5p normalization. The $2^{-\Delta\Delta CT}$ method was used to calculate the relative expression of target genes [29]. The primers and reaction conditions are listed in Supplementary table 2. All the samples were run in triplicate.

Western blot analysis

Whole cell lysates from the cell lines were prepared by lysing the cells in ice-cold RIPA buffer. Total cell lysates were prepared and 20 μg of proteins was subjected to Western blot analysis in 12% SDS–PAGE gels electrophoresis under denaturing and reducing conditions. Specific primary antibodies for SEMA3B (rabbit anti-human polyclonal antibody, ab48197; Abcam, UK), MLL4 (mouse anti-human monoclonal antibody, ab56770; Abcam, UK), and ZNF143 (rabbit anti-human polyclonal antibody, ab96650; Abcam, UK) were, respectively, used. GAPDH was used as a loading control.

Immunohistochemical staining assay

SEMA3B protein expression was detected by immunostaining using the avidin–biotin complex immunoperoxidase method, which was performed on paraffin-embedded tumor tissue section and corresponding normal tissue section. Rabbit anti-human polyclonal antibody for SEMA3B (1:100 dilution; Abcam, UK) was used to detect protein expression of SEMA3B. Scoring accounted for both representation of the areas and intensities of the stains. All of the slides were examined concurrently by three experienced pathologists, who were blinded to the clinical data.

Methylated CpG sites distribution via bisulfite genomic sequencing (BGS) method

Genomic DNA was extracted from cultured cell lines, frozen GCA tissues, and corresponding normal tissues using a simplified proteinase K digestion method. To examine the DNA methylation patterns, 1 μg of genomic DNA was bisulfite modified using Epitect Fast Bisulfite Conversion Kits (Qiagen, Germany) according to the manufacturer's protocol. The general methylated CpG site distribution in the five gastric cancer cell lines was detected by BGS assay. Two pairs of primers [region 1: for SEMA3B: from −126 to 173 bp (located in promoter to exon 1), for SEMA3B-AS1: from −359 to −61 bp; region 2: for SEMA3B: from 1406 to 1740 bp (located in intron 1 to exon 2), for SEMA3B-AS1: from −1592 to −1926 bp] were designed to recognize sodium bisulfite-converted DNA. Fifty ng of bisulfite-modified DNA was subjected to PCR amplification and the PCR products were cloned into pGEM-T vectors (Promega, Madison, WI, USA). 8–10 clones of each specimen were sequenced by automated fluorescence-based DNA sequencing.

Methylation analysis of the different regions via bisulfite conversion-specific and methylation-specific polymerase chain reaction (BS-MSP) method

According to the distribution of the main methylated CpG sites by BGS assay, the methylation status of two regions of SEMA3B (region 1: for SEMA3B: from −37 to 57 bp, for SEMA3B-AS1: from −243 to −150 bp; region 2: for SEMA3B: from 1459 to 1591 bp, for SEMA3B-AS1: from −1645 to −1777 bp) were respectively analyzed by BS-MSP method as previously described using bisulfite-treated genomic DNA. The primers and reaction conditions are listed in Supplementary table 2. The methylated genomic DNA treated by CpG methyltransferase (Sss I) (New England BioLabs, Beverly, MA, USA) in vitro was used as a positive control and water blank was used as a negative control. The reactions were performed in duplicate with each of the samples.

Luciferase constructs

To explore the transcriptional regulation of SEMA3B or SEMA3B-AS1, three promoter reporter plasmids of SEMA3B (pGL3-B1 spanned the −404 to 65 bp; pGL3-B2 spanned the −245 to 65 bp; pGL3-B3 spanned the −96 to 65 bp) and SEMA3B-AS1 (pGL3-S1 spanned the −452 to 59 bp; pGL3-S2 spanned the −251 to 59 bp; pGL3-S3 spanned the −91 to 59 bp) were constructed. To explore the regulation effect of miR-6872-5p on ZNF143 expression, the wild-type 3′-UTR pmirGLO-ZNF143 or diverse mutant pmirGLO-ZNF143-mut reporter plasmids were constructed. These recombination plasmids were then sequenced for confirmation.

Luciferase assay

1×10^5 BGC-823 cells per well were seeded in 24-well dish 24 h before transfection. In all, 200 ng of constructed reporter plasmids, pGL3-control vector (positive control) or pGL3-basic vector (negative control) constructs were cotransfected with 10 ng of pRL-TK vector using Lipofectamine 2000 (Invitrogen, Carlsbad, CA, USA). Luciferase activity was measured with the Dual-Luciferase Reporter Assay System (Promega, Madison, WI, USA). Promoter activities were expressed as the ratio of Firefly luciferase to Renilla luciferase activity. For the regulation effect of miR-6872-5p on ZNF143 transcriptional activity, the BGC-823 cells were transfected with either miR-6872-5p mimic (25 nM) or mimic control (25 nM) at 24 h after transfection with pmirGLO-ZNF143 or pmirGLO-ZNF143-mut reporter plasmids. After transfection for 48 h, the reporter luciferase activity was measured with the Dual-Luciferase Reporter assay system. Each data point was obtained in triplicate.

In vitro DNA methylation

Construct pGL3-B3 and pGL3-S2 were in vitro methylated as described previously [30]. Two hundred ng of mock or SSI-treated vector was transfected in BGC-823 cells. After 48 h, luciferase and Renilla activity were assayed as described above.

Chromatin immunoprecipitation (ChIP) assay

ChIP assay was carried out with EZ-Magna ChIP A/G (17-10086, Upstate, Millipore, MA, USA) according to the manufacturer's instructions. Antibodies against Sp1, MLL4, and H3K4me3, H3K9ac, and H3K9me2 within the SEMA3B promoter in BGC-823 cells (Upstate, Millipore, MA, USA) were used for immunoprecipitation. ChIP-derived DNA was quantified using real-time PCR analysis. The primers located in the promoter region of SEMA3B or SEMA3B-AS1 are shown in Supplementary table 2. Amplifications were performed in triplicate, and the enrichment was determined compared with input.

Cell transfection

For overexpression of SEMA3B and SEMA3B-AS1, the sequence of SEMA3B or SEMA3B-AS1 was synthesized and subcloned into pcDNA3.1 (Invitrogen, Carlsbad, CA, USA). The BGC-823 and MGC-803 cells were transfected with SEMA3B or SEMA3B-AS1 expression plasmid (pcDNA3.1-SEMA3B or pcDNA3.1-SEMA3B-AS1) or the empty vector (pcDNA3.1-EV) as control at a final concentration of 2 ug/uL using FuGENE HD Transfection Reagent (Promega, Madison, WI, USA). After transfection,

cells were incubated in antibiotic-free medium for 5 h, followed by replacement with fresh normal growth medium for a further incubation of 43 h by adding 800 µg/mL of G418 (Life Technologies, Carlsbad, CA, USA) to the supplemented culture medium. Resistant cell clones were isolated and expanded for further characterization. For inhibition of SEMA3B and SEMA3B-AS1, HGC-27 cells were respectively transfected with SEMA3B- or SEMA3B-AS1-specific shRNA plasmid using FuGENE HD Transfection Reagent, and a scrambled shRNA was used as a negative control. For overexpression of miR-6872-5p, BGC-823 and MGC-803 cells were transfected with miR-6872-5p mimic or mimic control (Ambion, Austin, TX, USA) at a final concentration of 25 nmol/L, and for downregulation of miR-6872-5p, HGC-27 cells were transfected with miR-6872-5p inhibitor or inhibitor control (Ambion, Austin, TX, USA).

Cell proliferation assay

The proliferation of SEMA3B- or SEMA3B-AS1-transfected BGC-823 and MGC-803 cells or shRNA-transfected HGC-27 cells was measured by cell-counting kit-8 (CCK-8) assay. Before proliferation was detected, 10 µl of CCK8 (Dojindo, Japan) was added to the 100 µl cultured cells, and after incubation for 2 h at 37 °C, the absorbance of each well was measured at a wavelength of 450 nm. All experiments were performed in triplicate.

Wound healing assay

Cell migration levels were determined by wound healing assay. A wound was produced by a straight scratch with a 200 µL pipette tip in the cultured cells, and then the images captured at the same position of each well 0 h, 12 h, and 24 h after the wound was created under a microscope. The relative distance of cell migration to the scratched area was measured and a healing percentage was calculated. The experiments were repeated in triplicate.

Cell invasion assay

The invasion ability of cells was evaluated in 24-well transwell chambers (Corning, Kennebunk, ME, USA). The transwell chambers were coated with 30 µg Matrigel and incubated at 37 °C for 1 h. The 5×10^4 cells/well were added in the upper chambers, and RPMI-1640 medium containing 10% FBS was added to the lower chambers. After 24 h at 37 °C, invasive cells located on the lower chamber were fixed with methanol and stained with crystal violet. The invaded cell numbers were counted in five microscopic fields (at ×100 magnification) per filter. The experiments were repeated in triplicate.

Subcellular fractionation

To determine the cellular localization of SEMA3B-AS1, cytoplasmic and nuclear RNA were isolated from HGC-27 and NCI-N87 cells using Nuclear/ Cytosol Fractionation Kit (BioVision, Milpitas, CA, USA) according to the manufacturer's instructions.

RNA immunoprecipitation assay

The binding of SEMA3B-AS1 to MLL4 was determined by RNA immunoprecipitation (RIP) assay using MLL4 antibody and the Magna RIP™ RNA-Binding Protein Immunoprecipitation Kit (Millipore, Billerica, MA, USA) according to the manufacturer's instructions. The IgG antibody was used as a negative control. The purified RNA was detected by qRT-PCR assay.

RNA pull-down assay

RNA pull-down assay was performed using Pierce Magnetic RNA–Protein Pull-Down Kit (Pierce Biotechnology, Rockford, IL, USA) in accordance with the manufacturer's instructions. Briefly, biotinylated SEMA3B-AS1 or antisense SEMA3B-AS1 was incubated with whole-cell lysates extracted from BGC-823 cells, and then complexes were isolated with streptavidin magnetic beads. The MLL4 protein present in the pull-down material was detected by western blot analysis.

Statistical analysis

Statistical analysis was performed with SPSS19.0 software package (SPSS Company, Chicago, Illinois, USA). The qRT-PCR results were expressed as the mean $\pm$ SD. Student's t test was used to compare the expression levels between different groups. The comparison of protein expression and methylation frequency between two groups was conducted using Pearson's Chi square test. Survival curves were made by using the Kaplan–Meier method, and the log-rank or the Breslow tests were used as needed for the univariate comparison of SEMA3B, SEMA3B-AS1, or miR-6872 expression and methylation categories. All statistical tests were two sided, and $P < 0.05$ was considered to be statistically significant.

Results

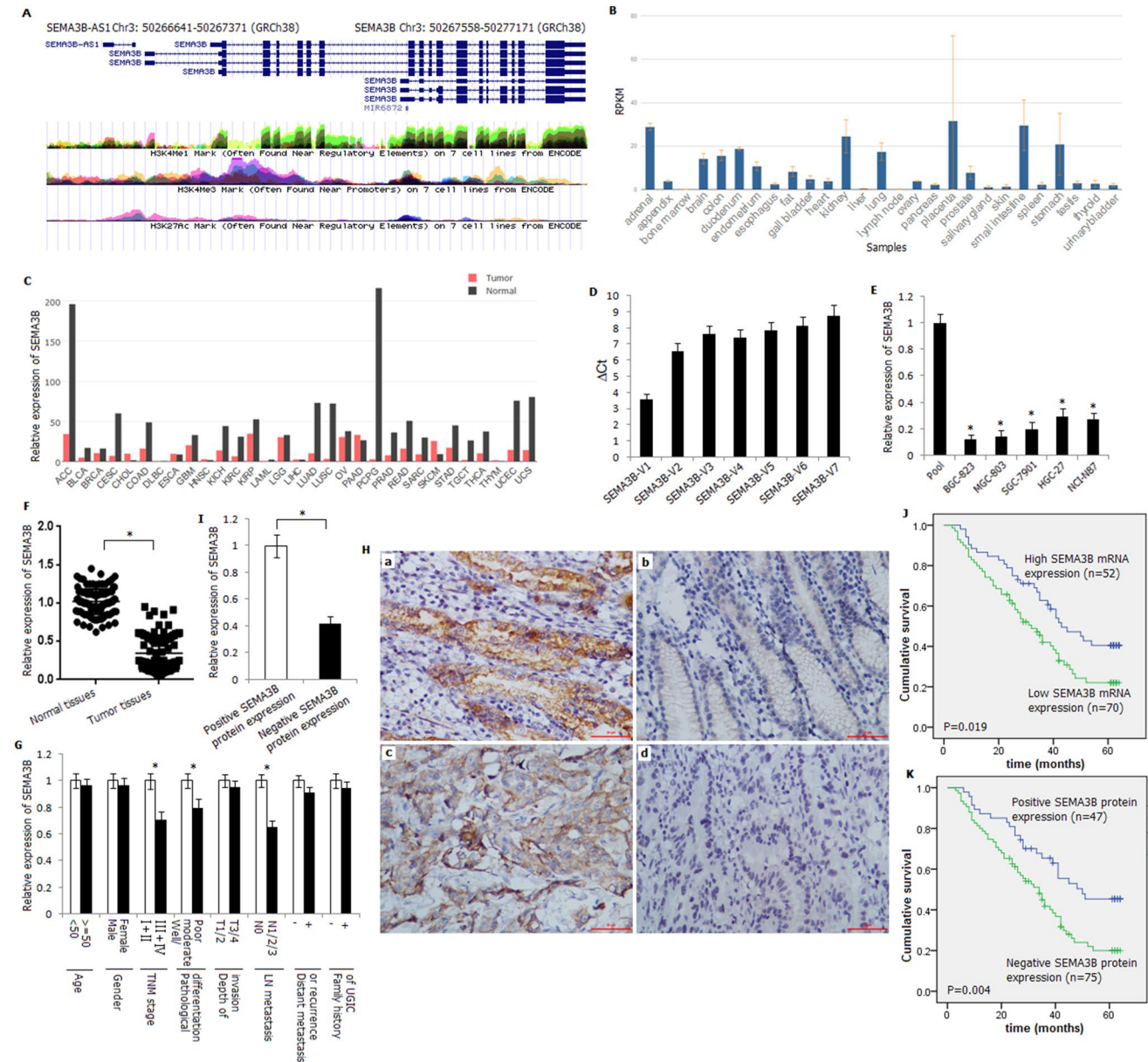## Downregulation of SEMA3B in GCA

The schematic representation of genomic organization of SEMA3B, SEMA3B-AS1, and miR-6872 is shown in Fig. 1a. There are seven transcripts of SEMA3B due to alternative splicing, and there are 187 base interval between the transcriptional start site of SEMA3B and SEMA3B-AS1. MiR-6872 is located at the intron of SEMA3B. We first scanned the relative expression level of SEMA3B in different normal tissues in the GENEBANK dataset and in various tumor types in the GEPIA dataset, and found relative high expression level of SEMA3B in stomach, adrenal, kidney, etc. (Fig. 1b), while the expression level of SEMA3B was downregulated in most of the tumor types (Fig. 1c). We examined the expression level of 7 transcripts of SEMA3B in normal tissues and identified that transcript 1 was the main transcript (Fig. 1d). We mainly focused on SEMA3B transcript 1 in the following studies.

A significantly decreased mRNA expression level of SEMA3B transcript 1 was detected in five gastric cancer cells (Fig. 1e). The mRNA expression level of SEMA3B in GCA tumor tissues was significantly decreased than in corresponding normal tissues ($P < 0.01$) (Fig. 1f). Among them, 70 patients (57.4%) demonstrated less than 50% expression level of SEMA3B in tumor tissues compared to the corresponding normal tissues. The expression level of SEMA3B in GCA tumor tissues was associated with TNM stage, pathological differentiation, and lymph node metastasis ($P < 0.05$) (Fig. 1g). The pattern of immunohistochemical staining of SEMA3B was cytoplasmic and nuclear, mainly cytoplasmic (Fig. 1h). Positive protein expression frequency of SEMA3B in tumor tissues (38.5%, 47/122) was significantly lower than that in corresponding normal tissues (79.5%, 97/122) ($P < 0.05$) (Supplementary table 3). SEMA3B protein expression was associated with TNM stage, pathological differentiation, and lymph node metastasis ($P < 0.05$) (Table 1). The mRNA expression level of SEMA3B in GCA patients with negative SEMA3B protein expression was decreased compared to that with positive SEMA3B protein expression (Fig. 1i). Survival analysis further verified that GCA patients with low SEMA3B mRNA expression level (the expression level of SEMA3B in the tumor tissues was less than 50% of that in corresponding normal tissues) or negative SEMA3B protein expression showed poorer survival rate (log-rank test, $P < 0.05$) (Fig. 1j, k).

Decreased expression of SEMA3B-AS1 in GCA

SEMA3B-AS1 has no open reading frame and coding capacity predicted by Coding Potential Calculator and Coding Potential Assessment Tool (Supplementary table 4). As shown in Fig. 2a, b, the expression trend of SEMA3B-AS1 in normal tissues in GENEBANK dataset and in various tumor types in GEPIA dataset was similar to SEMA3B, which demonstrated a relatively high expression level in normal tissues and downregulated in most of the tumor types. Similar

to the expression of SEMA3B, downregulation of SEMA3B-AS1 was also detected in gastric cancer cells and tumor tissues (Fig. 2c, d). Among them, 82 patients (67.2%) demonstrated less than 50% expression level of SEMA3B-AS1 in tumor tissues compared to the corresponding normal tissues. The expression level of SEMA3B-AS1 in GCA tumor tissues was associated with TNM stage, pathological differentiation, and lymph node metastasis ($P < 0.05$) (Fig. 2e). Survival analysis further verified that GCA patients with low SEMA3B-AS1 expression level (the expression level of SEMA3B-AS1 in the tumor tissues was less than 50% of that in corresponding normal tissues) showed poorer survival rate (log-rank test, $P < 0.05$) (Fig. 2f). Interestingly, the general expression level of SEMA3B-AS1 was lower when

compared with the mRNA expression level of SEMA3B either in normal tissues or in GCA tissues (Fig. 2g). However, the average fold change of SEMA3B-AS1 expression was higher than SEMA3B mRNA expression when GCA tissues compared to corresponding normal tissues. The mRNA expression level of SEMA3B was positively correlated with SEMA3B-AS1 in GCA tissues (Fig. 2h).

Upregulation of SEMA3B and SEMA3B-AS1 by 5-Aza-dC or TSA treatment in gastric cancer cells

Kuroki first detected the methylation status of intron 1 in SEMA3B [19], and most of the following research focused on the intronic CpG island methylation status [15, 18, 20].

◀**Fig. 1** The expression status of SEMA3B in GCA tissues and human gastric cancer cell lines. **a** Schematic representation of the genomic organization of SEMA3B, SEMA3B-AS1, and miR6872. **b** Relative expression of SEMA3B in different normal tissues detected by HPA RNA-seq in GENEBANK. **c** Relative expression of SEMA3B in various tumor types in GEPIA dataset. *ACC* adrenocortical carcinoma, *BLCA* bladder urothelial carcinoma, *BRCA* breast invasive carcinoma, *CESC* cervical squamous cell carcinoma and endocervical adenocarcinoma, *CHOL* cholangiocarcinoma, *COAD* colon adenocarcinoma, *DLBC* lymphoid neoplasm diffuse large B-cell lymphoma, *ESCA* esophageal carcinoma, *GBM* glioblastoma multiforme, *HNSC* head and neck squamous cell carcinoma, *KICH* kidney chromophobe, *KIRC* kidney renal clear cell carcinoma, *KIRP* kidney renal papillary cell carcinoma, *LAML* acute myeloid leukemia, *LGG* brain lower-grade glioma, *LIHC* liver hepatocellular carcinoma, *LUAD* lung adenocarcinoma, *LUSC* lung squamous cell carcinoma, *OV* ovarian serous cystadenocarcinoma, *PAAD* pancreatic adenocarcinoma, *PCPG* pheochromocytoma and paraganglioma, *PRAD* prostate adenocarcinoma, *READ* rectum adenocarcinoma, *SARC* sarcoma, *SKCM* skin cutaneous melanoma, *STAD* stomach adenocarcinoma, *TGCT* testicular germ cell tumors, *THCA* thyroid carcinoma, *THYM* thymoma, *UCEC* uterine corpus endometrial carcinoma, *UCS* uterine carcinosarcoma. **d** Expression levels of seven transcripts of SEMA3B in normal tissues. The results are shown as ΔCt values normalized to GAPDH. **e** Relative expression of SEMA3B in five human gastric cancer cell lines detected by qRT-PCR. Pools: average expression in 10 normal tissues was used as normal control. Asterisk, compared with pools, $P < 0.05$. **f** Relative expression of SEMA3B in GCA tissues and corresponding normal tissues detected by qRT-PCR. *$P < 0.05$. **g** Relative expression of SEMA3B in different subgroups. *$P < 0.05$. **h** immunohistochemical staining of SEMA3B in GCA tumor tissues and normal tissues (SP×400). a positive staining of SEMA3B in normal tissue; b negative staining of SEMA3B in normal tissue; c positive staining of SEMA3B in GCA tissue; d negative staining of SEMA3B in GCA tissue. **i** The correlation between mRNA and protein expression of SEMA3B. *$P < 0.05$. **j** Showing a direct correlation between low SEMA3B mRNA expression and poor patient survival. **k** Showing a direct correlation between negative SEMA3B protein expression and poor patient survival

Recently, Loginov [11, 31] detected the methylation of promoter CpG island was correlated with inactivation of SEMA3B. Based on the reported studies, we first analyzed the distribution of CpG islands of SEMA3B (Fig. 3a). We detected the methylation status of the promoter region and intron 1 of SEMA3B in the following studies. As shown in Fig. 3b, c, the expression levels of SEMA3B and SEMA3B-AS1 were significantly increased in the five gastric cancer cell lines after treatment with 5-Aza-dC and TSA, and the increased effect was more obvious after treatment with 5-Aza-dC + TSA.

Distribution of methylated CpG sites and aberrant methylation status of two regions in GCA

As shown in Fig. 3d, frequent methylation of the CpG sites within the two regions was observed by BGS assay in the gastric cancer cells. BS-MSP method was subsequently used to detect the methylation status of these CpG sites. As shown in Fig. 3e, methylation of region 1 and region 2 was detected

in gastric cancer cells and the methylation status of region 1 was completely reversed after 5-Aza-dC treatment. For primary GCA tissues and corresponding normal tissues, methylation frequency was 56.6% (69/122) and 10.7% (13/122) at region 1, 40.2% (49/122) and 29.5% (36/122) at region 2, respectively (Supplementary table 3). The methylation frequency of region 1 in GCA tissues was significantly higher than that in corresponding normal tissues ($P < 0.05$). The methylation status of region 1 in GCA tissues was associated with TNM stage, pathological differentiation, and lymph node metastasis ($P < 0.05$), while the methylation status of region 2 in GCA tissues was not associated with any clinicopathologic characteristics (Table 1).

The association of SEMA3B and SEMA3B-AS1 expression and methylation in GCA tissues

The mRNA expression level of SEMA3B in GCA tissues with hypermethylation of region 1 was significantly lower than that with unmethylation of the region ($P < 0.05$); however, the expression level was not associated with methylation status of region 2 ($P > 0.05$) (Fig. 3f). The protein expression level of SEMA3B was significantly correlated with region 1 methylation status and was not correlated with region 2 methylation status (Supplementary table 5). The expression level of SEMA3B-AS1 in GCA tissues with hypermethylation of region 1 was significantly lower than that with unmethylation of the region; however, it was not associated with region 2 methylation status ($P < 0.05$) (Fig. 3g).

Proximal promoter methylation of SEMA3B and SEMA3B-AS1 leads to a significant decrease in luciferase activity

To test the influence of promoter methylation on gene expression, different reporter constructs containing unmethylated promoter sequences of SEMA3B (pGL3-B1 to B3) and SEMA3B-AS1 (pGL3-S1 to S3) were made (Fig. 3h). As shown in Fig. 3i, j, pGL3-B3 and pGL3-S2 (spanning the same CpG sites of region 1) demonstrated the highest relative luciferase activity detected by the luciferase assay in BGC-823 cells, and further analysis showed significant decrease in luciferase activity of in vitro methylated pGL3-B3 and pGL3-S2 (Fig. 3K).

Sp1 activates SEMA3B or SEMA3B-AS1 transcription, and hypermethylation of the CpG sites within Sp1 binding sites eliminates Sp1 binding ability

We further scanned the potential transcription factor binding sites in the promoter region and found four Sp1 binding sites spanning −12 bp to 59 bp of SEMA3B or −245 bp to

Table 1 Protein expression and methylation status of SEMA3B in GCA tissues

| Group | N | Protein expression | | Methylation frequency | | | |
| | | | | Region 1 | | Region 2 | |
		n (%)	P	n (%)	P	n (%)	P
Age							
< 50	24	10(41.7)		13(54.2)		8(33.3)	
≥ 50	98	37(37.8)	0.724	56(57.1)	0.792	41(41.8)	0.446
Gender							
Male	99	39(39.4)		55(55.6)		39(39.4)	
Female	23	8(34.8)	0.682	14(60.9)	0.643	10(43.5)	0.719
TNM stage							
I+II	53	27(50.9)		22(41.5)		18(33.9)	
III+IV	69	20(29.0)	0.013	47(68.1)	0.003	31(44.9)	0.221
Pathological differentiation							
Well/moderate	78	36 (46.2)		38 (48.7)		30 (38.5)	
Poor	44	11 (25.0)	0.021	31 (70.5)	0.020	19 (43.2)	0.610
Depth of invasion							
T1/2	36	16 (44.4)		18 (50.0)		14 (38.9)	
T3/4	86	31 (36.0)	0.385	51 (59.3)	0.344	35 (40.7)	0.853
LN metastasis							
Negative (N0)	17	12 (70.6)		5 (29.4)		4 (23.5)	
Positive (N1/2/3)	105	35 (33.3)	0.003	64 (60.9)	0.015	45 (42.9)	0.132
Distant metastasis or recurrence							
Negative	53	23 (43.4)		27 (50.9)		19 (35.8)	
Positive	69	24 (34.8)	0.333	42 (60.9)	0.273	30 (43.5)	0.394
Family history of UGIC							
Negative	71	29 (40.8)		38 (53.5)		27 (38.0)	
Positive	51	18 (35.3)	0.534	31 (60.8)	0.425	22 (43.1)	0.570

− 175 bp of SEMA3B-AS1 (Fig. 3l). ChIP assay confirmed the binding of Sp1 to the four sites (Fig. 3m). The cotransfection of pGL3-B3 or pGL3-S2 and pcDNA3.1-Sp1 demonstrated the highest relative luciferase activity, indicating that Sp1 may upregulate SEMA3B or SEMA3B-AS1 transcription through directly binding to the Sp1 binding sites (Fig. 3n). The distribution of CG dinucleotide was found within the four Sp1 binding sites, and the influence of hypermethylation of these CG sites on Sp1 binding ability was further detected. As shown in Fig. 3o, Sp1 stimulation of the methylated pGL3-B3 and pGL3-S2 was much lower than that of the unmethylated constructs, suggesting that hypermethylation of the CG sites within the Sp1 binding sites which located around the transcription start site of SEMA3B or proximal promoter of SEMA3B-AS1 might abrogate Sp1 binding and transcriptional activation.

Histone modification regulates the expression of SEMA3B

We further detected the influence of histone modification on gene expression by real-time ChIP assay. As shown

in Fig. 3p–r, the active mark H3K4me3 and H3K9ac was much less than repressive mark H3K9me2 in the promoter region of SEMA3B. Increased degree of H3K4me3 and decreased degree of H3K9me2 were detected after the cells were treated with 5-Aza-dC. A significant enrichment of H3K9ac following the TSA treatment was observed in BGC-823 cells.

SEMA3B and SEMA3B-AS1 inhibit gastric cancer cell proliferation, migration, and invasion in vitro

The plasmid containing SEMA3B transcript (pcDNA3.1-SEMA3B) was then constructed and transfected into BGC-823 and MGC-803 cells. As shown in Fig. 4a, the expression level of SEMA3B was significantly upregulated in transfected BGC-823 and MGC-803 cells. The cell proliferation was significantly inhibited after BGC-823 and MGC-803 cells were transfected with pcDNA3.1-SEMA3B (Fig. 4b). Furthermore, overexpression of SEMA3B inhibited the migration and invasion of BGC-823 and MGC-803 cells in vitro (Fig. 4c, d). We further knocked down SEMA3B using short hairpin RNAs (shRNAs) in HGC-27 cells, and
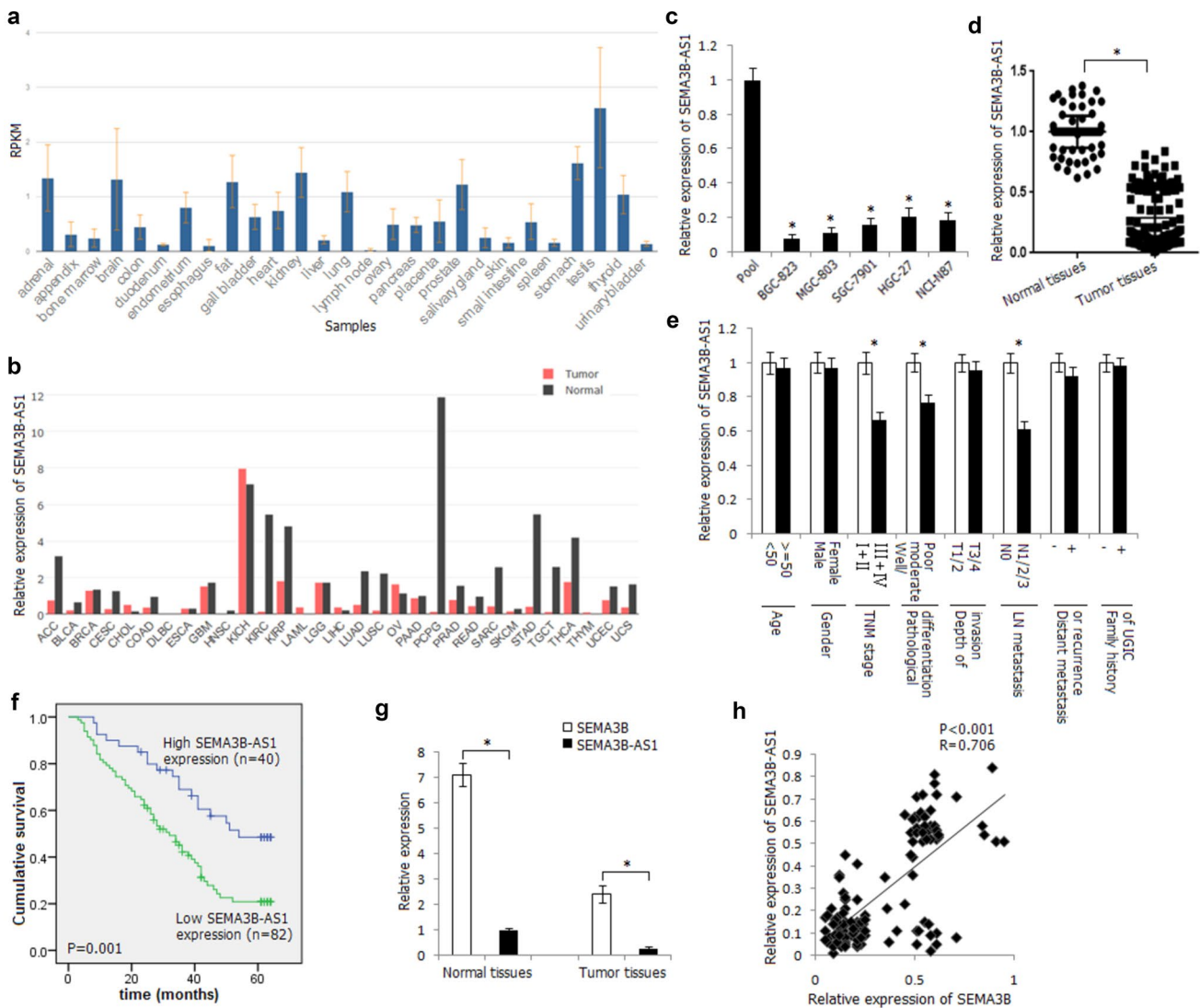
Fig. 2 The expression status of SEMA3B-AS1 in GCA tissues and human gastric cancer cell lines. **a** Relative expression of SEMA3B-AS1 in different normal tissues detected by HPA RNA-seq in GEN-EBANK. **b** Relative expression of SEMA3B-AS1 in various tumor types in the GEPIA dataset. **c** Relative expression of SEMA3B-AS1 in five human gastric cancer cell lines detected by qRT-PCR. Asterisk, compared with pools, $P < 0.05$. **d** Relative expression of SEMA3B-AS1 in GCA tissues and corresponding normal tissues detected by qRT-PCR. *$P < 0.05$. **e** Relative expression of SEMA3B-AS1 in different subgroups. *$P < 0.05$. **f** Showing a direct correlation between low SEMA3B-AS1 expression and poor patient survival. **g** Relative expression comparison of SEMA3B mRNA and SEMA3B-AS1 in GCA tissues and corresponding normal tissues. *$P < 0.05$. **h** The mRNA expression of SEMA3B in GCA tissues was positively correlated with the expression of SEMA3B-AS1

transfection of shRNA-SEMA3B-1 showed the strongest knock-down efficiency (Supplementary Fig. 1A). Transfection of shRNA-SEMA3B-1 in HGC-27 cells led to increased proliferation, migration, and invasion of the cells (Supplementary Fig. 1B, 1C, 1D).

We also constructed the plasmid containing the SEMA3B-AS1 transcript (pcDNA3.1-SEMA3B-AS1) and transfected into BGC-823 and MGC-803 cells. The expression level of SEMA3B-AS1 was significantly increased in the transfected cells (Fig. 4e) and overexpression of

SEMA3B-AS1 inhibited the proliferation, migration, and invasion of BGC-823 and MGC-803 cells in vitro (Fig. 4f–h). The expression level of SEMA3B-AS1 was also knocked down using shRNAs in HGC-27 cells, and transfection of shRNA-SEMA3B-AS1-2 demonstrated the strongest knock-down efficiency (Supplementary Fig. 2A). Transfection of shRNA-SEMA3B-AS1-2 in HGC-27 cells led to increased proliferation, migration, and invasion of the cells (Supplementary Fig. 2B–D).
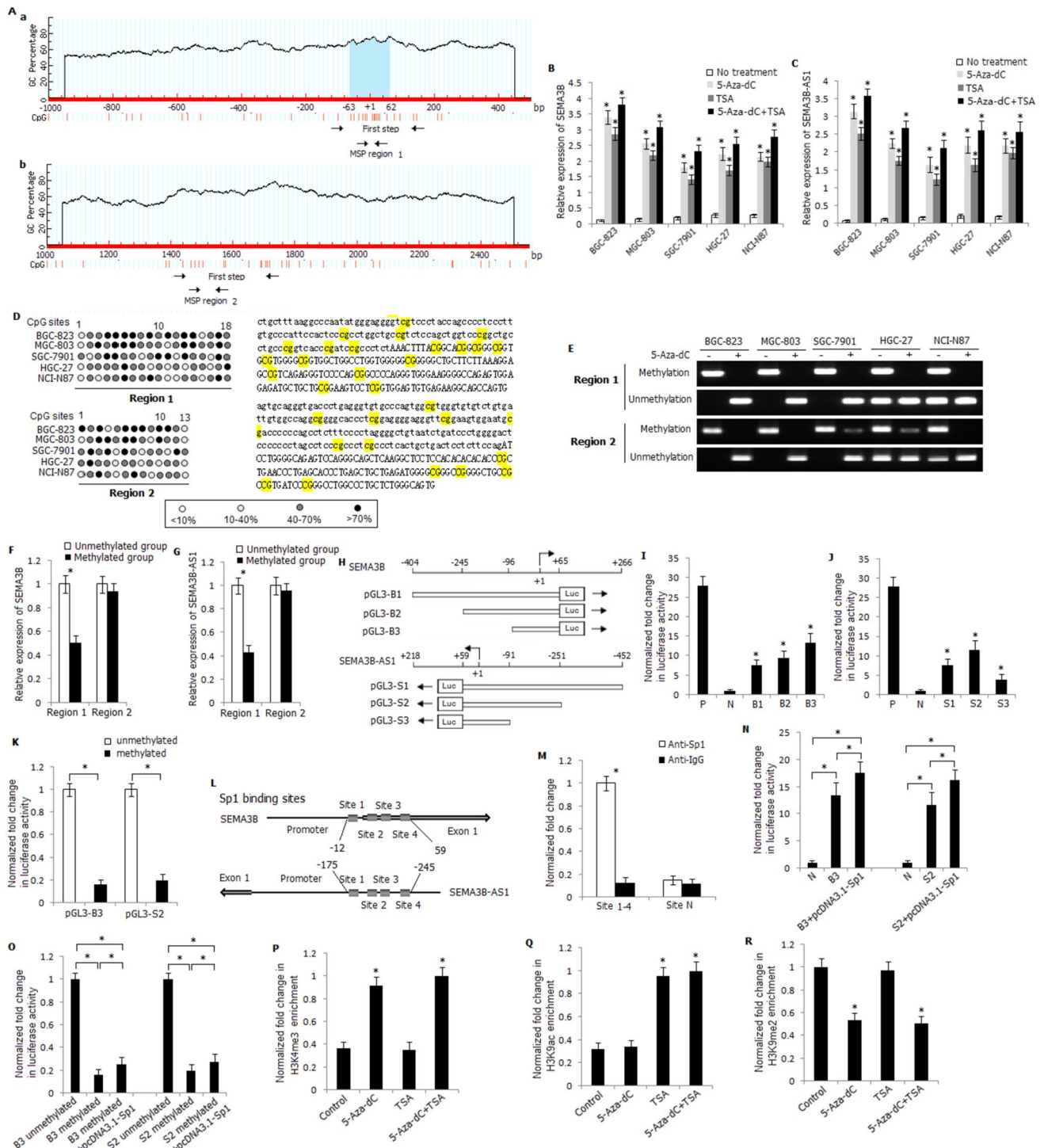
SEMA3B-AS1 upregulates SEMA3B expression by interacting with MLL4

As shown in lncATLAS (http://lncatlas.crg.eu), SEMA3B-AS1 was mainly located in the nucleus of Hela.S3 cells and cytoplasm of MCF.7 cells (Fig. 5a), and SEMA3B-AS1 was both located in cytoplasm and nucleus as predicted by lncLocator (Supplementary table 6). In the present study, SEMA3B-AS1 was detected both in the cytoplasm and nucleus, mainly in the nucleus (Fig. 5b). Overexpression of SEMA3B-AS1 increased the mRNA expression level of SEMA3B in BGC-823 and MGC-803 cells (Fig. 5c); however, overexpression of SEMA3B had no influence on the expression level of SEMA3B-AS1 (Fig. 5d). Knock-down

◄Fig. 3 The epigenetic regulation of SEMA3B and SEMA3B-AS1 transcription. **a** Schematic structure of SEMA3B CpG islands predicted by MethPrimer. a One CpG island is located in the regions spanning the proximal promoter to exon 1 of SEMA3B. b No apparent CpG islands are predicted in the regions spanning intron 1 to exon 2 of SEMA3B. MSP regions analyzed are indicated in the different regions. **b** Relative expression of SEMA3B in gastric cancer cells treated or not treated with 5-Aza-dC, TSA, and 5-Aza-dC+TSA detected by qRT-PCR. Asterisk, compared with untreated cells, $P < 0.05$. **c** Relative expression of SEMA3B-AS1 in gastric cancer cells treated or not treated with 5-Aza-dC, TSA, and 5-Aza-dC+TSA detected by qRT-PCR. * Compared with untreated cells, $P < 0.05$. **d** High-resolution mapping of the methylation status of every CpG site in the two regions by BGS assay in the five gastric cancer cell lines. Each CpG site is shown at the top row as an individual number. Percentage methylation was determined as percentage of methylated cytosines from 8 to 10 sequenced colonies. The color of circles for each CpG site represents the percentage of methylation. **e** The methylation status of the two regions in gastric cancer cell lines treated or not treated with 5-Aza-dC by BS-MSP analysis. **f** Relative expression of SEMA3B in the tumor tissues with and without methylation of the two regions. *$P < 0.05$. **g** Relative expression of SEMA3B-AS1 in the tumor tissues with and without methylation of the two regions. *$P < 0.05$. **h** The relative position and construction of reporter vectors of SEMA3B and SEMA3B-AS1. **i** Luciferase activity of reporter constructs of SEMA3B in BGC-823 cells. The pGL3-control vector was used as a positive (P), and empty pGL3-basic vector as a negative control (N). pGL3-B3 showed the highest relative luciferase activity. Astersik compared with N, $P < 0.05$. **j** Luciferase activity of reporter constructs of SEMA3B-AS1 in BGC-823 cells. Astersik compared with N, $P < 0.05$. **k** The pGL3-B3 and pGL3-S2 were in vitro methylated, cloned into pGL3 vector and luciferase activity was determined and compared with that of unmethylated pGL3-B3 and pGL3-S2. *$P < 0.05$. **l** The relative location of Sp1 binding sites in the promoter region of SEMA3B and SEMA3B-AS1 predicted by PROMO. **m** ChIP assay in 5-Aza-dC-treated HGC-27 cells using anti-Sp1, or nonspecific IgG. Enrichment was determined relative to input controls. Site N was used as negative control with no binding sites for Sp1. Data are mean ± SD of $n = 3$ independent experiments. *$P < 0.05$. **n** Dual luciferase reporter assays were used to determine the Sp1 binding on the SEMA3B and SEMA3B-AS1 promoter region in BGC-823 cells. *$P < 0.05$. **o** Sp1 and methylation status affected the promoter activity. *$P < 0.05$. **p–r**. A real-time ChIP assay was used to determine the enrichment of H3K4me3 (**p**), H3K9ac (**q**), and H3K9me2 (**r**) within the SEMA3B promoter in BGC-823 cells. Asterisk, compared with untreated cells, $P < 0.05$

of SEMA3B-AS1 led to decreased expression level of SEMA3B in HGC-27 cells (Fig. 5e); however, knock-down of SEMA3B had no influence on SEMA3B-AS1 expression level in HGC-27 cells (Fig. 5f). Overexpression of SEMA3B-AS1 also increased the protein expression level of SEMA3B in BGC-823 and MGC-803 cells, and knock-down of SEMA3B-AS1 decreased the protein expression level of SEMA3B in HGC-27 cells (Fig. 5g). Co-overexpression of SEMA3B and SEMA3B-AS1 significantly inhibited the proliferation and invasion of BGC-823 and MGC-803 cells than the effect of individual overexpression of SEMA3B or SEMA3B-AS1, and knock-down of SEMA3B in the BGC-823 and MGC-803 cells with overexpression of SEMA3B-AS1 attenuated the inhibitory effect (Fig. 5h, i).

SEMA3B-AS1 was mainly located in the nucleus of cells, so we considered if SEMA3B-AS1 regulated the expression of SEMA3B in nucleus by binding some proteins, such as transcription factors, or epigenetic regulation enzymes. Abundant H3K4me3 signals are clustered in the promoter region of SEMA3B (Fig. 1a), indicating that SEMA3B may be regulated by histone methylation. Myeloid/lymphoid or mixed-lineage leukemia (MLL) family genes are the mostly important enzymes that modify H3K4 methylation [32, 33]. We predicted the binding ability of MLL1 to MLL5 with SEMA3B-AS1 by RPISeq and found the greatest interaction probability between MLL4 protein and SEMA3B-AS1 (RF: 0.7 and SVM: 0.93). RNA immunoprecipitation assay demonstrated the binding of SEMA3B-AS1 with MLL4 protein in SEMA3B-AS1-transfected BGC-823 cells (Fig. 5j). RNA pull-down assay also showed the binding of SEMA3B-AS1 with MLL4 (Fig. 5k). Co-expression of SEMA3B-AS1 and MLL4 had a synergistic promoting effect on the mRNA and protein overexpression of SEMA3B (Fig. 5l, m). Furthermore, real-time ChIP assay revealed that overexpression of SEMA3B-AS1 increased the enrichment of MLL4 and the level of H3K4me3 at the promoter region of SEMA3B (Fig. 5n).

Downregulation of miR-6872 in GCA

We further investigated whether SEMA3B and miR-6872 are transcribed together in GCA. We scanned the expression status of miR-6872-5p in YM500v2 miR-Seq database and found lower expression level of miR-6872-5p in most of the tumor types, including stomach cancer (Fig. 6a), and the general expression level of miR-6872-5p in tumors was lower (Fig. 6b). Downregulation of miR-6872-5p was also detected in gastric cancer cells and tumor tissues (Fig. 6c, d). Sixty-six patients (54.1%) demonstrated less than 50% expression level of miR-6872-5p in tumor tissues compared with the corresponding normal tissues. The expression level of miR-6872-5p in GCA tumor tissues was associated with TNM stage, pathological differentiation, and lymph node metastasis ($P < 0.05$) (Fig. 6e). Moreover, GCA patients with low miR-6872-5p expression level (the expression level of miR-6872-5p in the tumor tissues was less than 50% of that in corresponding normal tissues) demonstrated poorer survival rate (log-rank test, $P < 0.05$) (Fig. 6f). Furthermore, the expression level of miR-6872-5p was positively correlated with the expression level of SEMA3B in GCA tissues (Fig. 6g).

The transcription of miR-6872-5p is regulated by DNA methylation and histone modification

As shown in Fig. 6h, significant upregulation of miR-6872-5p was detected after the cells were treated with
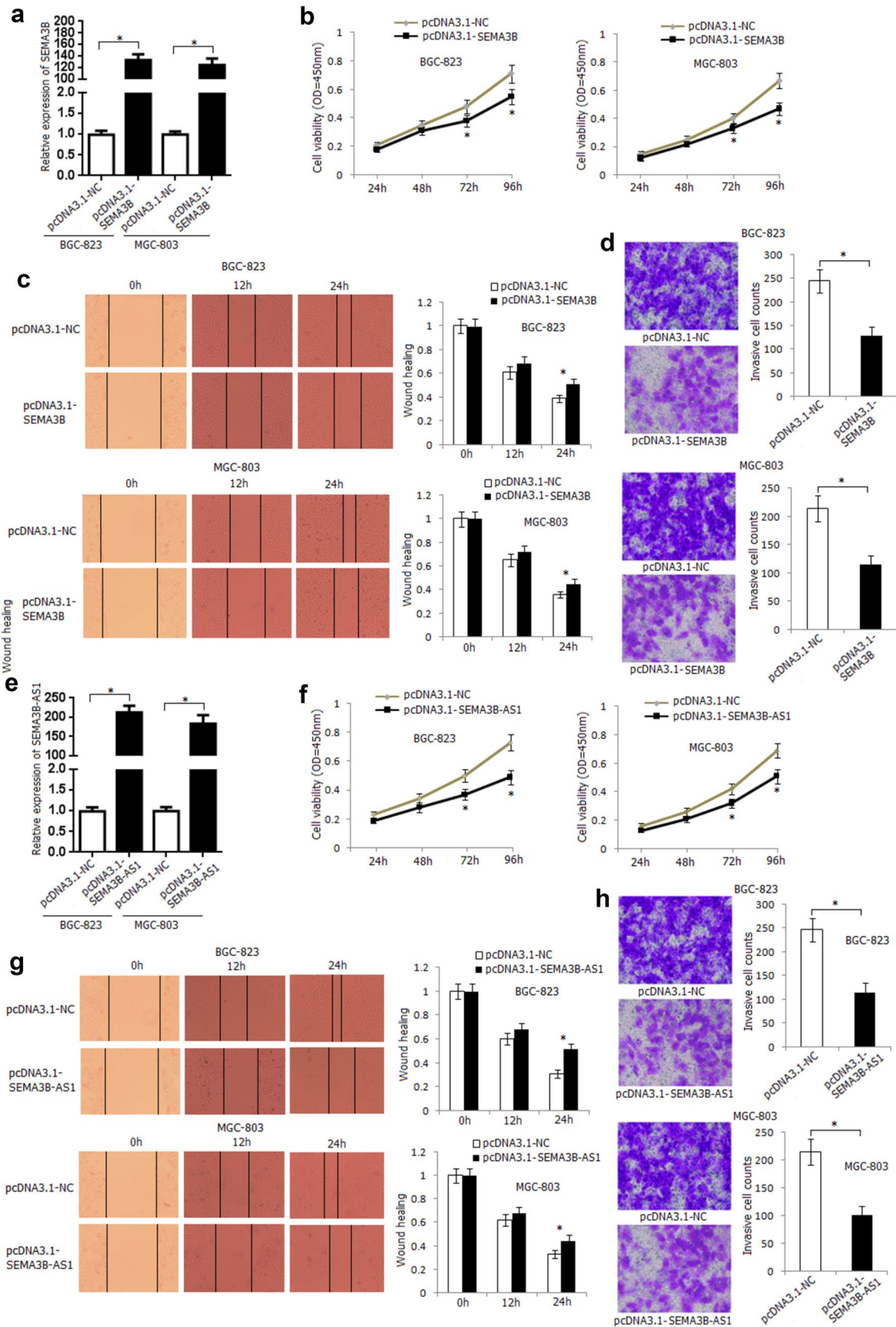
◀**Fig. 4** The functional analysis of SEMA3B and SEMA3B-AS1 in human gastric cancer cell lines. **a** Upregulation of SEMA3B was detected by qRT-PCR in SEMA3B-transfected BGC-823 and MGC-803 cells compared with empty vector-transfected cells. *$P < 0.05$. **b** Overexpression of SEMA3B inhibited BGC-823 and MGC-803 cell proliferation. Asterisk, compared with empty vector, $P < 0.05$. **c** Overexpression of SEMA3B inhibited the migration of BGC-823 and MGC-803 cells detected by wound healing assay. Asterisk, compared with empty vector, $P < 0.05$. **d** Overexpression of SEMA3B inhibited the invasiveness of BGC-823 and MGC-803 cells detected by transwell invasion assay. Asterisk, compared with empty vector, $P < 0.05$. **e** Upregulation of SEMA3B-AS1 was detected by qRT-PCR in SEMA3B-AS1-transfected BGC-823 and MGC-803 cells. Asterisk, compared with empty vector-transfected cells, $P < 0.05$. **f** Overexpression of SEMA3B-AS1 inhibited BGC-823 and MGC-803 cell proliferation. Asterisk, compared with empty vector, $P < 0.05$. **g** Overexpression of SEMA3B-AS1 inhibited the migration of BGC-823 and MGC-803 cells detected by wound healing assay. Asterisk, compared with empty vector, $P < 0.05$. **h** Overexpression of SEMA3B-AS1 inhibited the invasiveness of BGC-823 and MGC-803 cells detected by transwell invasion assay. Asterisk, compared with empty vector, $P < 0.05$. For all quantitative results, the data are presented as the mean ± SD. The experiments are representative of three independent experiments with similar results

5-Aza-dC or TSA, and the effect was more obvious after the cells were treated with 5-Aza-dC + TSA. Furthermore, the relative expression level of miR-6872-5p in GCA tissues with hypermethylation of region 1 was significantly lower than that with unmethylation of the region; however, it was not associated with region 2 methylation status ($P < 0.05$) (Fig. 6i).

miR-6872-5p functions synergistically with its host gene SEMA3B to suppress cell migration and invasion

The BGC-823 and MGC-803 cells were transfected with miR-6872-5p mimics and HGC-27 cells were transfected with miR-6872-5p inhibitor, and the transfection efficiency was verified by the qRT-PCR method (Fig. 6j and Supplementary Fig. 3A). As shown in Fig. 6j, enhanced expression level of SEMA3B did not appreciably affect the level of miR-6872-5p; similarly, the expression level of SEMA3B was not influenced by miR-6872-5p overexpression in BGC-823 and MGC-803 cells. Overexpression or knock-down of miR-6872-5p significantly suppressed or increased the cell invasion (Fig. 6k and Supplementary Fig. 3B); furthermore, the co-elevated expression level of SEMA3B and miR-6872-5p resulted in a further decrease in the cell invasion of BGC-823 and MGC-803 cells (Fig. 6k).

ZNF143 is the target gene of miR-6872-5p in GCA

After prediction by TargetScan and miRDB, ZNF143 may be the candidate target gene and the binding sites are shown in Fig. 6l. The mRNA expression of ZNF143 in GCA tissues

was significantly higher than that in corresponding normal tissues (Fig. 6m). Overexpression or knock-down of miR-6872-5p suppressed or increased the mRNA and protein expression level of ZNF143 (Fig. 6n, o, Supplementary Fig. 3C, D), and overexpression of miR-6872-5p suppressed the luciferase activity after BGC-823 cells were transfected with luciferase reporters containing ZNF143 3′-UTR (Fig. 6p). Overexpression of SEMA3B or SEMA3B-AS1 did not influence the mRNA expression of ZNF143 (Fig. 6q, r).

Discussion

Several class 3 semaphorins such as semaphorin 3B and semaphorin 3F have been characterized as tumor suppressors [34]. The tumor suppressor role of SEMA3B has been confirmed both in vitro and in vivo in some tumor types [11–13, 35]. Approximately, 37% of mammalian miRNA genes appeared to be intronic miRNA genes [36], and about 94.2% of predicted promoter regions of intronic miRNA genes overlapped with promoters of their host genes [37]. Moreover, the majority of mammalian intronic miRNA genes are found to be frequently co-expressed with their protein-coding host genes under the promoter-driven regulation of the host gene [38]. As a kind of lncRNAs, antisense lncRNAs are transcribed from the opposite position of their sense protein coding genes, and many antisense lncRNAs may regulate the expression and function of the sense genes in cis [39]. In the present study, a similar expression trend of SEMA3B, SEMA3B-AS1, and miR-6872-5p was detected in GCA tissues and they might have a suppressor role through suppressing gastric cancer cell proliferation, migration, and invasion. Furthermore, the association of their expression with GCA patients' prognosis suggested their vital roles as prognostic biomarkers in GCA.

SEMA3B methylation has been observed in various types of cancers, including gallbladder carcinoma, lung cancer, and glioma [12, 15, 18–20]. These studies only focused on the methylation status of the CpG sites within the first intron of SEMA3B. However, there is a true promoter region, which includes CpG-dinucleotides with higher density and is capable of binding transcription factors, such as Sp1. Loginov et al. subsequently studied the promoter methylation status of SEMA3B in lung and renal cancers and found frequent methylation of intronic and promoter CpG islands in both lung and renal primary tumors, and the methylation frequency detected in the promoter CpG island was higher than that in the intronic island. In addition, an association was observed between the decrease of the SEMA3B mRNA level and the methylation of the promoter CpG island [11, 31]. In the present study, frequent methylation of the promoter and intronic CpG islands in GCA tissues was detected,
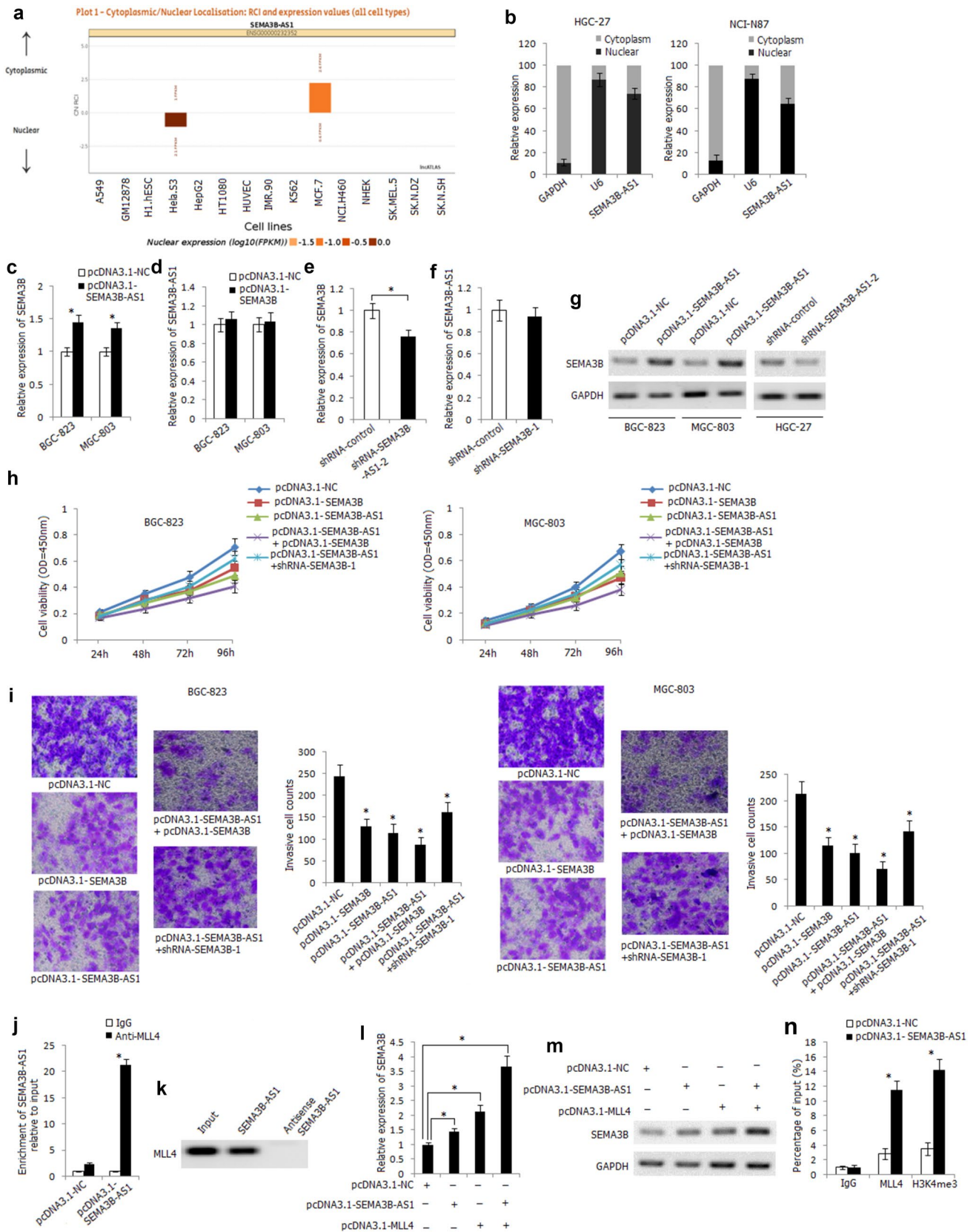
◄**Fig. 5** SEMA3B-AS1 upregulates SEMA3B expression through interacting with MLL4. **a** Subcellular localization of SEMA3B-AS1 in various cells predicted by lncATLAS. **b** The levels of SEMA3B-AS1 in nuclear and cytoplasmic fractions of HGC-27 and NCI-N87 cells detected by qRT-PCR. *GAPDH* cytoplasmic control; *U6* nuclear control. **c** Overexpression of SEMA3B-AS1 increased the expression of SEMA3B in SEMA3B-AS1-transfected BGC-823 and MGC-803 cells. Asterisk, compared with empty vector, $P < 0.05$. **d** Overexpression of SEMA3B has no influence on SEMA3B-AS1 expression. **e** Knock-down of SEMA3B-AS1 decreased the expression of SEMA3B in shRNA-SEMA3B-AS1-2-transfected HGC-27 cells. Asterisk, compared with shRNA control, $P < 0.05$. **f** Knock-down of SEMA3B has no influence on SEMA3B-AS1 expression in shRNA-SEMA3B-1-transfected HGC-27 cells. **g** Protein expression of SEMA3B was detected by Western blot assay in pcDNA3.1-SEMA3B-AS1-transfected BGC-823 and MGC-803 cells or in shRNA-SEMA3B-AS1-2-transfected HGC-27 cells. **h** The BGC-823 and MGC-803 cell proliferation in different transfected groups. **i** The BGC-823 and MGC-803 cell invasive ability in different transfected groups. Asterisk, compared with empty vector, $P < 0.05$. **j** RIP assay showed the binding of SEMA3B-AS1 with MLL4 in SEMA3B-AS1-transfected BGC-823 cells. **k** RNA pull-down assay showed the binding of SEMA3B-AS1 with MLL4. **l** Co-expression of SEMA3B-AS1 and MLL4 had a synergistic promoting effect on the mRNA upregulation of SEMA3B. **m** Co-expression of SEMA3B-AS1 and MLL4 had a synergistic promoting effect on the protein overexpression of SEMA3B. **n** Real-time ChIP assay revealed that overexpression of SEMA3B-AS1 increased the enrichment of MLL4 and the level of H3K4me3 at the promoter region of SEMA3B. Asterisk, compared with empty vector, $P < 0.05$

and the methylation frequency of promoter region was found to be significantly higher in GCA tissues than that in corresponding normal tissues and the promoter region methylation was observed to be associated with the expression level of SEMA3B, SEMA3B-AS1 and miR-6872-5p. Combined with further luciferase activity analysis, implied the important role of promoter methylation on SEMA3B, SEMA3B-AS1, and miR-6872-5p inactivation.

Aberrant CpG island hypermethylation may directly or indirectly affect the binding of specific transcription factors and subsequently influence gene transcription. Four transcription factor Sp1 binding sites, including CG dinucleotides, are predicted within the CpG island of the promoter region. Our further analyses verified that the hypermethylation of these CG dinucleotides affected the binding ability

of Sp1 to the binding sites and led to the transcriptional repression of SEMA3B.

A large amount of antisense lncRNAs can regulate the expression of sense protein coding genes in cis, and in the present study SEMA3B-AS1 was detected to induce the expression of SEMA3B by interacting with MLL4 to increase the enrichment of MLL4 and H3K4me3 at the promoter region of SEMA3B. MLL4 is necessary to maintain broad H3K4me3 and super-enhancers at tumor suppressor genes [32]. In the current study, SEMA3B-AS1 was detected to combine directly with MLL4 by RIP and RNA pull-down assay, and further increased the accumulation of MLL4 and H3K4me3 at the promoter region of SEMA3B, suggesting that SEMA3B-AS1 plays an important role in maintaining the activation status of SEMA3B.

As an intronic miRNA, the role of miR-6872-5p in tumorigenesis has not been fully clarified. Downregulation of miR-6872-5p was detected in GCA tissues and gastric cancer cells and miR-6872-5p might act as tumor-suppressive miRNA to function synergistically with its host gene SEMA3B. Furthermore, ZNF143 might be the target gene of miR-6872-5p. ZNF143 regulates many cell cycle-associated genes. ZNF143 is expressed strongly in gastric cancer tissues and enhanced gastric cancer cell migration by promoting the process of EMT through PI3K/AKT signaling pathway [40]. Although miR-6872-5p cannot regulate the expression of its host gene, miR-6872-5p may function synergistically with SEMA3B by targeting ZNF143 to suppress migration and invasion of GCA.

In summary, SEMA3B, SEMA3B-AS1, and miR-6872-5p play tumor-suppressive roles in GCA tumorigenesis, and their expression levels are coregulated by promoter aberrant hypermethylation and histone modification. SEMA3B-AS1 induces the expression of SEMA3B by interacting with MLL4. ZNF143 is the target gene of miR-6872-5p, and miR-6872-5p functions synergistically with SEMA3B to suppress cancer cell invasion. Moreover, SEMA3B, SEMA3B-AS1, and miR-6872-5p may serve as potential prognostic markers in predicting GCA patients' survival.
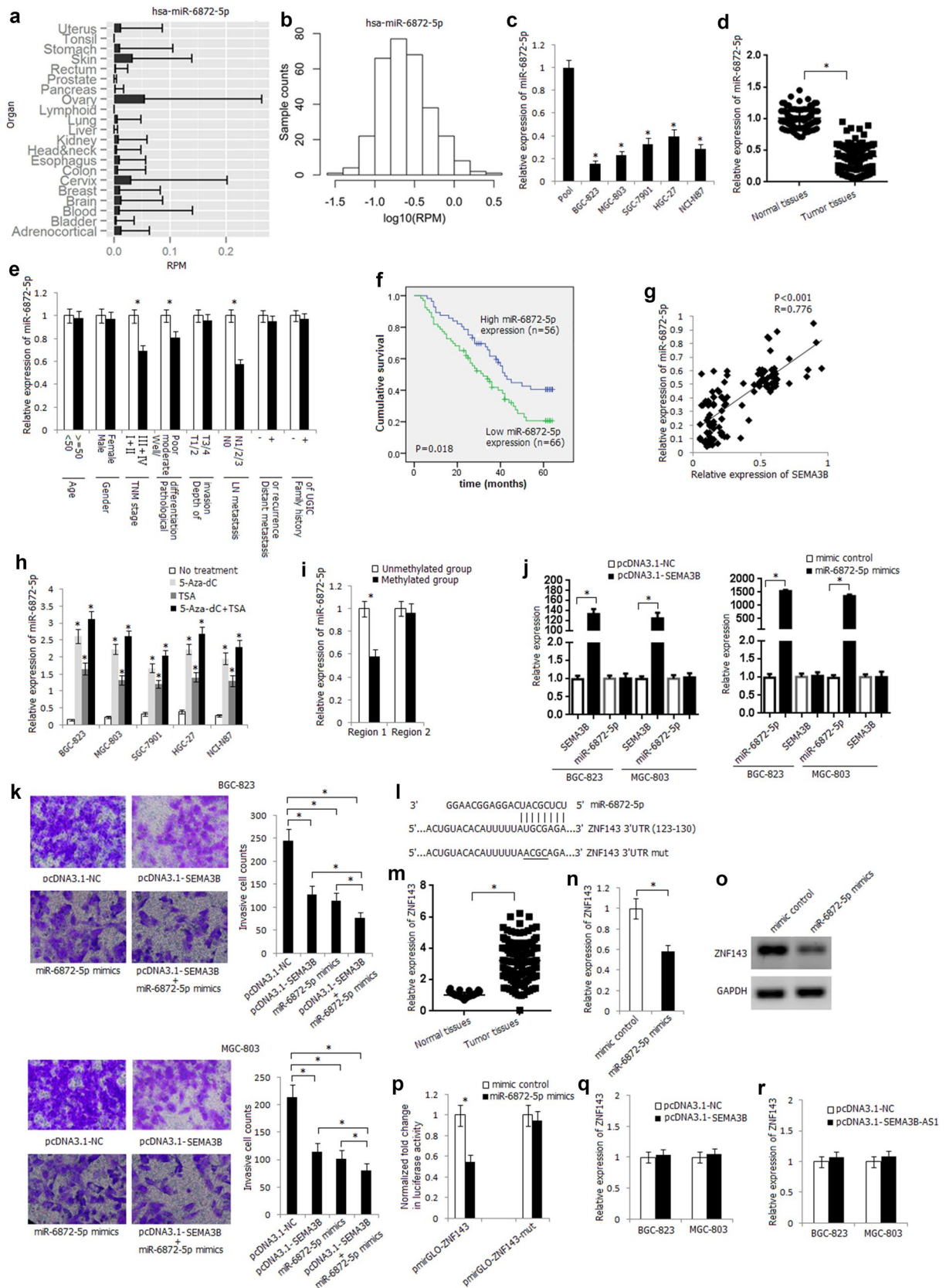
◄**Fig. 6** SEMA3B functions synergistically with miR-6872-5p to suppress gastric cancer cell migration. **a** The expression status of miR-6872-5p in different tumor types in YM500v2 miR-Seq database. **b** The expression distributions of miR-6872-5p in tumors in YM500v2 miR-Seq database. **c** Relative expression of miR-6872-5p in human gastric cancer cell lines detected by qRT-PCR. * Compared with pools, $P < 0.05$. **d** Relative expression of miR-6872-5p in GCA tissues and corresponding normal tissues. *$P < 0.05$. **e** Relative expression of miR-6872-5p in different subgroups. *$P < 0.05$. **f** Showing a direct correlation between low miR-6872-5p expression and poor patient survival. **g** The expression of SEMA3B in GCA tissues was positively correlated with the expression of miR-6872-5p. **h** Relative expression of miR-6872-5p in gastric cancer cells treated or untreated with 5-Aza-dC, TSA, and 5-Aza-dC+TSA detected by qRT-PCR. Asterisk, compared with untreated cells, $P < 0.05$. **i** Relative expression of miR-6872-5p in the tumor tissues with and without methylation of the two regions. *$P < 0.05$. **j** Expression of SEMA3B and miR-6872-5p following overexpression of SEMA3B and miR-6872-5p in BGC-823 and MGC-803 cells. *$P < 0.05$. **k** Co-transfection of pcDNA3.1-SEMA3B and miR-6872-5p mimics significantly inhibited the invasiveness of BGC-823 and MGC-803 cells detected by transwell invasion assay. *$P < 0.05$. **l** Schematic diagram of potential miR-6872-5p target sites in ZNF143 3′-UTR. **m** Relative mRNA expression of ZNF143 in GCA tissues and corresponding normal tissues. *$P < 0.05$. **n** Upregulation of miR-6872-5p decreased the mRNA expression of ZNF143 in BGC-823 cells. Asterisk, compared with mimic control, $P < 0.05$. O. Upregulation of miR-6872-5p decreased the protein expression of ZNF143 in BGC-823 cells. **p** Luciferase activity in BGC-823 cells transfected with luciferase reporters containing ZNF143 3′-UTR or ZNF143 3′-UTR mut. *$P < 0.05$. **q** The mRNA expression of ZNF143 following overexpression of SEMA3B in BGC-823 and MGC-803 cells. **r** The mRNA expression of ZNF143 following overexpression of SEMA3B-AS1 in BGC-823 and MGC-803 cells

Compliance with ethical standards

Conflict of interest The authors declare that they have no conflicts of interest.

Ethical approval The study was approved by the Ethics Committee of the Fourth Hospital, Hebei Medical University.

Informed consent Informed consent was obtained from all participants included in the study.

References

1. Vial M, Grande L, Pera M. Epidemiology of adenocarcinoma of the esophagus, gastric cardia, and uppergastric third. Recent Results Cancer Res. 2010;182:1–17.
2. Torre LA, Bray F, Siegel RL, Ferlay J, Lortet-Tieulent J, Jemal A. Global cancer statistics, 2012. CA Cancer J Clin. 2015;65:87–108.
3. Chow WH, Finkle WD, McLaughlin JK, Frankl H, Ziel HK, Fraumeni JF. The relation of gastroesophageal reflux disease and its treatment to adenocarcinomas of the esophagus and gastric cardia. JAMA. 1995;274:474–7.
4. Wang LD, Zheng S, Zheng ZY, Casson AG. Primary adenocarcinomas of lower esophagus, esophagogastric junction and gastric cardia: in special reference to China. World J Gastroenterol. 2003;9:1156–64.
5. Plummer M, Franceschi S, Vignat J, Forman D, de Martel C. Global burden of gastric cancer attributable to *Helicobacter pylori*. Int J Cancer. 2015;136:487–90.
6. Wistuba II, Behrens C, Virmani AK, Mele G, Milchgrub S, Girard L, et al. High resolution chromosome 3p allelotyping of human lung cancer and preneoplastic/preinvasive bronchial epithelium reveals multiple, discontinuous sites of 3p allele loss and three regions of frequent breakpoints. Cancer Res. 2000;60:1949–60.
7. Lerman MI, Minna JD. The 630-kb lung cancer homozygous deletion region on human chromosome 3p21.3: identification and evaluation of the resident candidate tumor suppressor genes. The international lung cancer chromosome 3p21.3 Tumor Suppressor Gene Consortium. Cancer Res. 2000;60:6116–33.
8. Chen J, Brevet A, Blanquet S, Plateau P. Control of 5′,5′-dinucleoside triphosphate catabolism by APH1, a Saccharomyces cerevisiae analog of human FHIT. J Bacteriol. 1998;180:2345–9.
9. Yue W, Dacic S, Sun Q, Landreneau R, Guo M, Zhou W, et al. Frequent inactivation of RAMP2, EFEMP1 and Dutt1 in lung cancer by promoter hypermethylation. Clin Cancer Res. 2007;13:4336–44.
10. Guo W, Dong Z, Chen Z, Yang Z, Wen D, Kuang G, et al. Aberrant CpG Island hypermethylation of RASSF1A in gastric cardia adenocarcinoma. Cancer Invest. 2009;27:459–65.
11. Loginov VI, Dmitriev AA, Senchenko VN, Pronina IV, Khodyrev DS, Kudryavtseva AV, et al. Tumor suppressor function of the SEMA3B Gene in human lung and renal cancers. PLoS One. 2015;10:e0123369.
12. Pang CH, Du W, Long J, Song LJ. Mechanism of SEMA3B gene silencing and clinical significance in glioma. Genet Mol Res. 2016. https://doi.org/10.4238/gmr.15017664.
13. Castro-Rivera E, Ran S, Brekken RA, Minna JD. Semaphorin 3B inhibits the phosphatidylinositol 3-kinase/Akt pathway through neuropilin-1 in lung and breast cancer cells. Cancer Res. 2008;68:8295–303.
14. Chen R, Zhuge X, Huang Z, Lu D, Ye X, Chen C, et al. Analysis of SEMA3B methylation and expression patterns in gastric cancer tissue and cell lines. Oncol Rep. 2014;31:1211–8.
15. Riquelme E, Tang M, Baez S, Diaz A, Pruyas M, Wistuba II, et al. Frequent epigenetic inactivation of chromosome 3p candidate tumor suppressor genes in gallbladder carcinoma. Cancer Lett. 2007;250:100–6.
16. Luo Y, Raible D, Raper JA. Collapsin: a protein in brain that induces the collapse and paralysis of neuronal growth cones. Cell. 1993;75:217–27.
17. Gaur P, Bielenberg DR, Samuel S, Bose D, Zhou Y, Gray MJ, et al. Role of class 3 semaphorins and their receptors in tumor growth and angiogenesis. Clin Cancer Res. 2009;15:6763–70.
18. Grote HJ, Schmiemann V, Geddert H, Rohr UP, Kappes R, Gabbert HE, et al. Aberrant promoter methylation of p16(INK4a), RARB2 and SEMA3B in bronchial aspirates from patients with suspected lung cancer. Int J Cancer. 2005;116:720–5.
19. Kuroki T, Trapasso F, Yendamuri S, Matsuyama A, Alder H, Williams NN, et al. Allelic loss on chromosome 3p21.3 and promoter hypermethylation of semaphorin 3B in non-small cell lung cancer. Cancer Res. 2003;63:3352–5.
20. Ito M, Ito G, Kondo M, Uchiyama M, Fukui T, Mori S, et al. Frequent inactivation of RASSF1A, BLU, and SEMA3B on 3p21.3 by promoter hypermethylation and allele loss in non-small cell lung cancer. Cancer Lett. 2005;225:131–9.

21. Bartel DP. MicroRNAs: genomics, biogenesis, mechanism, and function. Cell. 2004;116:281–97.

22. Gao X, Qiao Y, Han D, Zhang Y, Ma N. Enemy or partner: relationship between intronic micrornas and their host genes. IUBMB Life. 2012;64:835–40.

23. Taft RJ, Pang KC, Mercer TR, Dinger M, Mattick JS. Non-coding RNAs: regulators of disease. J Pathol. 2010;220:126–39.

24. Iyer MK, Niknafs YS, Malik R, Singhal U, Sahu A, Hosono Y, et al. The landscape of long noncoding RNAs in the human transcriptome. Nat Genet. 2015;47:199–208.

25. Schmitt AM, Chang HY. Long noncoding RNAs in cancer pathways. Cancer Cell. 2016;29:452–63.

26. Amin V, Harris RA, Onuchic V, Jackson AR, Charnecki T, Paithankar S, et al. Epigenomic footprints across 111 reference epigenomes reveal tissue-specific epigenetic regulation of lincRNAs. Nat Commun. 2015;6:6370.

27. Wang Z, Yang B, Zhang M, Guo W, Wu Z, Wang Y, et al. LncRNA epigenetic landscape analysis identifies EPIC1 as an oncogenic lncRNA that interacts with MYC and promotes cell-cycle progression in cancer. Cancer Cell. 2018;33:706–20.

28. Siewert JR, Stein HJ. Classification of adenocarcinoma of the oesophagogastric junction. Br J Surg. 1998;85:1457–9.

29. Livak KJ, Schmittgen TD. Analysis of relative gene expression data using real-time quantitative PCR and the 2(-Delta Delta C(T)) method. Methods. 2001;25:402–8.

30. Yu L, Liu C, Vandeusen J, Becknell B, Dai Z, Wu YZ, et al. Global assessment of promoter methylation in a mouse model of cancer identifies ID4 as a putative tumor-suppressor gene in human leukemia. Nat Genet. 2005;37:265–74.

31. Loginov VI, Khodyrev DS, Pronina IV, Maliukova AV, Kazubskaia TP, Ermilova VD, et al. Two CpG-islands of SEMA3B gene: methylation in clear cell renal cell carcinoma. Mol Biol (Mosk). 2009;43:1088–92.

32. Dhar SS, Zhao D, Lin T, Gu B, Pal K, Wu SJ, et al. MLL4 Is Required to Maintain Broad H3K4me3 Peaks and Super-Enhancers at Tumor Suppressor Genes. Mol Cell. 2018;70:825–41.

33. Ananthanarayanan M, Li Y, Surapureddi S, Balasubramaniyan N, Ahn J, Goldstein JA, et al. Histone H3K4 trimethylation by MLL3 as part of ASCOM complex is critical for NR activation of bile acid transporter genes and is downregulated in cholestasis. Am J Physiol Gastrointest Liver Physiol. 2011;300:G771–81.

34. Neufeld G, Kessler O. The semaphorins: versatile regulators of tumour progression and tumour angiogenesis. Nat Rev Cancer. 2008;8:632–45.

35. Tse C, Xiang RH, Bracht T, Naylor SL. Human Semaphorin 3B (SEMA3B) located at chromosome 3p21.3 suppresses tumor formation in an adenocarcinoma cell line. Cancer Res. 2002;62:542–6.

36. Griffiths-Jones S, Grocock RJ, van Dongen S, Bateman A, Enright AJ. miRBase: microRNA sequences, targets and gene nomenclature. Nucleic Acids Res. 2006;34:D140–4.

37. Wang G, Wang Y, Shen C, Huang YW, Huang K, Huang TH, et al. RNA polymerase II binding patterns reveal genomic regions involved in microRNA gene regulation. PLoS One. 2010;5:e13798.

38. Baskerville S, Bartel DP. Microarray profiling of microRNAs reveals frequent coexpression with neighboring miRNAs and host genes. RNA. 2005;11:241–7.

39. Bach DH, Lee SK. Long noncoding RNAs in cancer cells. Cancer Lett. 2018;419:152–66.

40. Wei S, Wang L, Zhang L, Li B, Li Z, Zhang Q, et al. ZNF143 enhances metastasis of gastric cancer by promoting the process of EMT through PI3K/AKT signaling pathway. Tumour Biol. 2016;37:12813–21.